Materials Research Bulletin 45 (2010) 1375–1382

Contents lists available at ScienceDirect

Materials Research Bulletin

journal homepage: www.elsevier.com/locate/matresbu

Synthesis and characterization of mesoporous-TiO_2 with enhanced photocatalytic activity for the degradation of chloro-phenol

Sajjad Shamaila [a], Ahmed Khan Leghari Sajjad [a], Feng Chen [a], Jinlong Zhang [a,b,*]

[a] *Key Laboratory for Advanced Materials and Institute of Fine Chemicals, East China University of Science and Technology, 130 Meilong Road, Shanghai 200237, PR China*
[b] *School of Chemistry and Materials Science, Guizhou Normal University, Guiyang 550001, PR China*

ARTICLE INFO

Article history:
Received 28 March 2010
Received in revised form 26 May 2010
Accepted 18 June 2010
Available online 25 June 2010

Keywords:
A. Nanostructures
A. Oxide
B. Sol–gel chemistry
D. Catalytic properties

ABSTRACT

Mesoporous-titania (TiO_2) photocatalysts have been synthesized using polyethylene glycol (PEG) as a template in dilute acetic acid aqueous solution by hydrothermal process. The effect of PEG molecular weights and thermal treatment on the resultant structure and photocatalytic activity are investigated. Structural and phase compositional properties of the resultant photocatalysts are characterized by transmission electron microscopy, X-ray diffraction and nitrogen sorption analysis. When the molecular weights of PEG vary from 600 to 20,000, the particle sizes of mesoporous structure decrease from 15.1 to 13.3 nm and mean pore sizes increase from 6.9 to 10.6 nm. The chemical reactions of the formation of mesoporous-TiO_2 during its synthesis have been proposed and discussed. The activities of mesoporous-TiO_2 photocatalysts are evaluated and compared with Degussa P-25 using chloro-phenol as a testing compound. The reaction mechanism of photodegradation is also described on the basis of high performance liquid chromatography.

1. Introduction

Metal oxide functional materials, especially titanium dioxide have been a hot topic of interest to researchers in many different fields due to enormous potential applications of such materials as membranes, solar energy conversion, chemical sensors and catalysis [1–7]. Among these, mesoporous titanium dioxide is of great interest because this class of materials possesses well-defined porous sizes, porosity and large specific surface areas [8,9]. When these are used as photocatalysts for degradation of organics, these desirable properties are anticipated to improve the activity because the performances of such photocatalysts rely on these attributes [3,4,8,9]. During the past two decades, many synthetic methods have been proposed to obtain mesoporous titanium dioxide including sol–gel, template assisted, hydrothermal, solvothermal, ultrasound-induced, ion liquid and evaporation-induced self-assembly [10–16]. Among these methods, the sol–gel is probably the simplest method but formation of aggregated nanoparticles during the precipitation and post-calcination processes often leads to poorly defined mesoporous structures [17]. In order to obtain well-defined mesoporous structures and better control on porous size and porosity of the resultant material, various structural directing reagents have been introduced to sol–gel processes. Among all the used surfactants, polyethylene glycol (PEG) is a nondegradable and hydrophilic polymer that can be crosslinked into hydrogels through various chemistry methods. PEG-based hydrogels were developed by introducing terminal acrylate functional groups which could take part in photopolymerization reactions [18,19]. PEG has been frequently used as a structure-directing reagent to obtain nanoporous SiO_2 [8,20,21], aluminosilicate [22,23] and other composite materials [15]. However, only a limited number of investigations have been reported to produce mesoporous-TiO_2 by employing PEG as the structural directing reagent [9,24–26].

In the traditional sol–gel method for TiO_2 preparation, it is often difficult to control the rate of hydrolysis because titanium precursors are highly reactive towards water. As a result, the physicochemical properties of TiO_2 have been practically uncontrollable. Several attempts have been made to solve this problem. In practice, strong acids (i.e. HCl and HNO_3) and complex reagents (i.e. acetylacetone, oxalate and citrate) are commonly employed to reduce the rapidity of the hydrolysis process [27,28]. When a strong acid is employed, the pH of the reaction solution changes rapidly with time which may lead to formation of less porous and larger particle-sized TiO_2 [29]. Weak acid such as acetic acid (HAc) has been used to replace strong acids because it control the hydrolysis process of titanium sources due to the chelating effect of acetic anions and formation of pH buffer [12,25]. In this preparation method, it is possible to control the physical properties

---

[*] Corresponding author at: Key Laboratory for Advanced Materials and Institute of Fine Chemicals, East China University of Science and Technology, Shanghai 200237, PR China. Tel.: +86 21 64252062; fax: +86 21 64252062.
E-mail address: jlzhang@ecust.edu.cn (J. Zhang).

0025-5408/$ – see front matter © 2010 Elsevier Ltd. All rights reserved.
doi:10.1016/j.materresbull.2010.06.047

of the resulting materials including surface area, particle size and pore structure by adjusting preparation variables.

Chlorinated phenols widely used as pesticides, herbicides and wood preservatives, are among the top priority pollutants and found in aqueous ecosystems as byproducts of chlorinated water. Moreover, chlorinated phenols are chemical precursors of the more toxic polychlorinated dibenzo-p-dioxins [30]. Due to this, chloro-phenol was employed as an environmentally relevant model pollutant. The chloro-phenol was degraded in an illuminated suspension of TiO_2 according to the following stoichiometry:

$$2C_6H_4OHCl + 13O_2 \xrightarrow{TiO_2/h\nu} 2HCl + 12CO_2 + 4H_2O$$

In this work, we report the preparation of mesoporous-TiO_2 by employing PEG with different molecular weights and acetic acid, as the structural directing reagent and hydrolytic retardants, respectively. The procedure involves a post-hydrothermal treatment to improve the quality of the resultant mesoporous-TiO_2. The effects of molecular weight of PEG, hydrothermal treatment and calcination temperatures are studied in comparison to control the physical properties of the resulting materials including surface area, particle size and pore structure (structural characteristics) of the resultant mesoporous-TiO_2. The mechanism of chemical reactions involved in the synthesis of mesoporous-TiO_2 and degradation of chloro-phenol has also been proposed.

2. Experimental

2.1. Materials

Tetrabutyl titanate (TBT) $Ti(OBu)_4$, PEG with different molecular weights, absolute ethanol and acetic acid (HAc) were analytical grade. All the above chemicals were purchased from Shanghai Sinopharm Chemical Reagent Co., Ltd., China. Deionized and doubly distilled water was used throughout the experiment.

2.2. Catalyst preparation

Mesoporous-TiO_2 was prepared using the hydrothermal-assisted sol–gel method. In a typical synthesis procedure 5.0 g of TBT was added drop-by-drop to 30 mL of acetic acid aqueous solution (20%, v/v) under vigorous stirring. The mixed solution was sealed and stirring was continued for 4 h to obtain solution A. In a separate beaker, 3.0 g of PEG with the molecular weight of 600 (designated as PEG 600) was dissolved in 20 mL ethanol under vigorous stirring to obtain solution B. Solution B was then added drop-by-drop to solution A. The final mixed solution was sealed and stirred for 24 h at room temperature. The resultant solution was then transferred into a Teflon sealed container for hydrothermal treatment under a constant temperature of 140 °C for 48 h. The precipitations were then collected and dried overnight in air at 80 °C. The as-prepared sample was then subjected to a thermal treatment process at 450 °C for 4 h. To examine the effect of calcination temperature, the as-prepared sample was also calcined at different temperatures. Furthermore, in order to evaluate the effect of the molecular weight of PEGs, we replaced the PEG 600 by 2000, 10,000 and 20,000, respectively.

2.3. Characterization

The crystal phase composition and crystallinity of the obtained mesoporous-TiO_2 was determined by X-ray diffraction (XRD) with Rigaku D/Max 2550 VB/PC apparatus (Cu Kα radiation, $\lambda = 0.154056$ nm) at room temperature operated at 40 kV and 100 mA. Diffraction patterns were recorded in the angular range of 20–80°. The crystallite size was estimated by applying the Scherrer equation to the full width at half-maximum (fwhm) of the (1 0 1) peak of anatase. $D = K\lambda/\beta\cos\theta$. Where β is the half-height width of the diffraction peak of anatase, $K = 0.89$ is a coefficient, θ is the diffraction angle and λ is the X-ray wavelength corresponding to the Cu Kα irradiation. The morphology was studied using scanning electron microscopy (SEM) (JEOL, JSM-6360LV) and transmission electron microscopy (TEM, JEM-2011) with an accelerating voltage of 200 kV. Nitrogen adsorption and desorption isotherms were obtained at 77 K with a Micromeritics ASAP 2010 system. All the samples were degassed at 473 K before the measurement. Fourier transform infrared (FT-IR) spectra were carried out by employing a Nicolet 740 FT-IR spectrometer equipped with a TGS detector and a KBr beam splitter.

2.4. Measurements of photocatalytic activities

Chloro-phenol was chosen as a model pollutant to evaluate the photocatalytic activities. The photocatalytic reactions were carried out at 30 °C using a home-made reactor. A high-pressure Hg lamp of 300 W having the strongest emission wavelength of 365 nm, was used as a UV light source (the average light intensity was about 1230 $\mu W/cm^2$). It was mounted 10 cm away from the reaction solution. During the reaction, a water-cooling system cooled the water-jacketed photochemical reactor to maintain the solution at room temperature. The photocatalyst (1.5 g L^{-1}) was added into a 100 mL quartz photoreactor containing 50 mL of a 50 mg L^{-1} aqueous solution of chloro-phenol. The mixture was sonicated for 20 min and stirred for 30 min in the dark in order to reach the adsorption–desorption equilibrium. Under UV irradiation and vigorous stir, each reaction was lasted for 5 h. Preliminary studies indicated a linear light absorbance verse chloro-phenol concentration and that the decomposition of chloro-phenol in the absence of photocatalyst or UV irradiation could be neglected.

To analyze the concentration of chloro-phenol and degradation products, the suspension was first centrifuged and filtered through 0.22 μm Millipore membrane filters to remove the catalyst. The membrane filters are made of mixed cellulose esters and had no effect on chloro-phenol concentration. The concentrations of chloro-phenol were measured with a UV–vis spectrophotometer (Varian Cary 100) with UV absorbance in the range of 200–400 nm and the UV λ_{max} value of chloro-phenol is 280 nm corresponded to the maximal adsorption of chloro-phenol. The concentrations of chloro-phenol were calculated from the height of peak by using calibration curve. The measurements were repeated for the catalyst and the experimental error was found to be within ±3%.

Chloro-phenol degradation intermediates were determined by the HPLC series 1100 (Agilent) equipped with a reverse-phase C18 analytical column (Zorbax SB-C18, USA) of 150 mm × 2.1 mm and 3.5 μm particle diameter. Column temperature was maintained at 22 °C. The mobile phase used for eluting chloro-phenol from the HPLC columns consisted of methanol and water (50:50, v/v) at a flow-rate of 1.0 mL min^{-1}.

3. Results and discussion

Mesoporous-TiO_2 was synthesized by using PEG as template and acetic acid a weak acid for the formation of smaller and uniform titanium hydrate. Fine mesoporous-TiO_2 particles during the hydrolysis process were obtained due to the better control of the hydrolysis process of titanium source, chelating effect of acetic anions and formation of pH buffer [31,32]. The post-hydrothermal treatment was performed to increase the crystallinity of mesoporous-TiO_2 [33]. Mesoporous-TiO_2 materials were found to have a high crystallinity with a nanocrystalline anatase structure. The addition of PEG with higher molecular weight enlarged the mesopore size and widened the mesopore size distribution of the material.

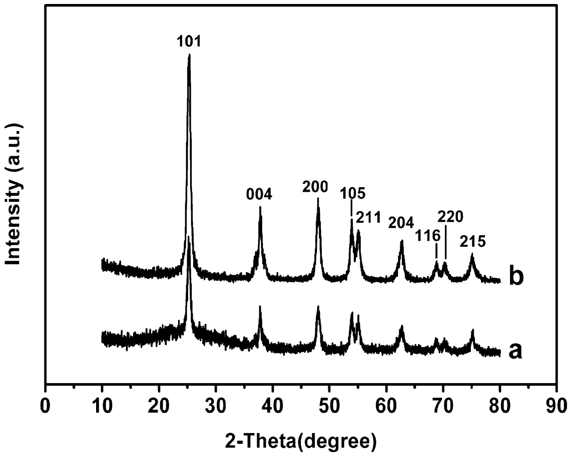

Fig. 1. XRD patterns obtained from samples (a) without hydrothermal treatment and (b) with hydrothermal treatment prepared by PEG 600 and calcined at 450 °C.

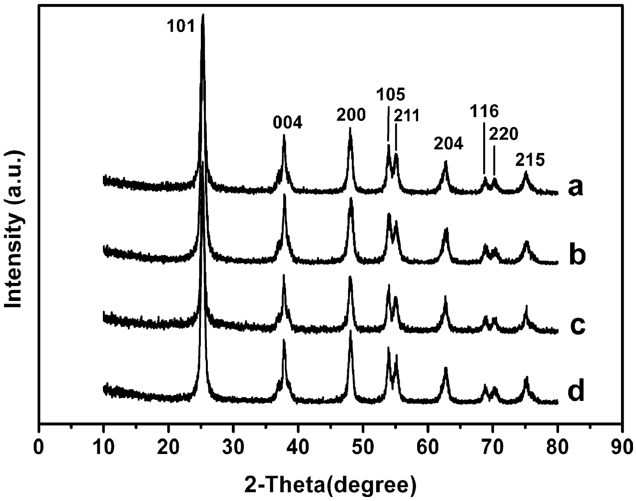

Fig. 2. XRD patterns of samples prepared with different molecular weights of PEG calcined at 450 °C (a) PEG 600; (b) PEG 2000; (c) PEG 10,000; (d) PEG 20,000.

3.1. X-ray diffraction spectroscopy

The wide angle XRD patterns of mesoporous-TiO_2 prepared with and without hydrothermal treatment are presented in Fig. 1. The samples exhibit characteristic anatase peaks which can be indexed to 25.3 (1 0 1), 37.2 (0 0 4), 48.9 (2 0 0), 54.0 (1 0 5), 55.3 (2 1 1), 62.4 (2 0 4) and 68.7 (1 1 6) (JCPDS no. 21-1272) and suggest that anatase is the highly crystalline phase [5,34]. The mean crystal sizes of the resultant mesoporous-TiO_2 were calculated from the broadening of the (1 0 1) XRD peak of anatase phase according to the Scherrer formula [35]. The mean crystal sizes of 15.0 and 16.4 nm were obtained from samples with and without hydrothermal treatment, respectively.

The effect of molecular weights of PEG on the mean crystalline size of the hydrothermally treated samples was investigated as shown in Fig. 2. These samples were calcined at 450 °C for 4 h. It was found that the mean crystalline sizes decreased from 15.0 to 13.3 nm when the molecular weight increased from 600 to 20,000 (see Table 1). These results are in agreement with the report [5]. The wide angle XRD patterns of hydrothermally treated mesoporous-TiO_2 calcined at different temperatures were recorded and given in Fig. 3. The anatase was found to be the only crystalline phase present in all samples regardless of the treatment temperature up to 600 °C. As expected, an increase in the treatment temperature resulted in an increase in the crystallinity. The mean crystalline sizes calculated from the XRD patterns were found to be increased from 9.8 to 36 nm with the temperature treatment up to 600 °C.

3.2. N_2 adsorption–desorption

Fig. 4 shows the N_2 sorption isotherms of mesoporous-TiO_2 samples prepared with different PEG molecular weights. All isotherms reveal Type IV curve with a small H_2 hysteresis loop which are characteristics of mesoporous structure [36]. A sharp increase in the amount of adsorbed N_2 was recorded with samples prepared by different PEG molecular weights from 600 to 20,000. The effect of PEG molecular weight on the pore size distribution was also investigated (the inset Fig. 4). It was found that an increase in the PEG molecular weight leads to a stepwise increase in the pore size distribution. For the PEG molecular weights of 600–20,000, the observed pore size distribution was ranged from 6.9 to 10.6 nm. Interestingly, this stepwise increasing trend caused by the PEG molecular size was also observed for the pore volume (Table 1).

3.3. Scanning electron microscopy

The effect of PEG addition on surface microstructure of mesoporous-TiO_2 was investigated by scanning electron microscopy. Fig. 5a shows the SEM image of the mesoporous-TiO_2 prepared by using PEG 600 which consists of irregular shaped primary particles. It is observed that sample has granular texture with uniform pores at the surface as shown in Fig. 5b. It is therefore concluded that the sample prepared by addition of PEG is porous in nature.

3.4. Transmission electron microscopy

The TEM image of mesoporous-TiO_2 sample calcined at 450 °C for 4 h is shown in Fig. 6. The TEM image of the particles reveals the mesostructure without long range order in titania particles. The entire matrix between the mesopores is composed of anatase crystalline nanodomains of about 14–15 nm in size. This corresponds well with the domain size (ca. 15 nm) obtained from XRD. Fig. 6b is a local enlarged TEM image of Fig. 6a. The presence of clearly resolved lattice fringes demonstrates that the framework of

Table 1
Structural parameters of mesoporous-TiO_2 prepared with PEG of different molecular weights.

Samples	Phase of formation	Particle size (nm)[a]	S_{BET} (m^2/g)[b]	Pore size (nm)[c]	Pore volume ($cm^3 g^{-1}$)[d]
PEG 600	A	15.1	71	6.87	0.18
PEG 2000	A	14.2	90	7.20	0.21
PEG 10,000	A	13.9	95	7.61	0.23
PEG 20,000	A	13.3	106	10.6	0.29

[a] Calculated by the Scherrer equation.
[b] BET surface area calculated from the linear part of the BET plot.
[c] Estimated using the desorption branch of the isotherm.
[d] Estimated by BJH method.

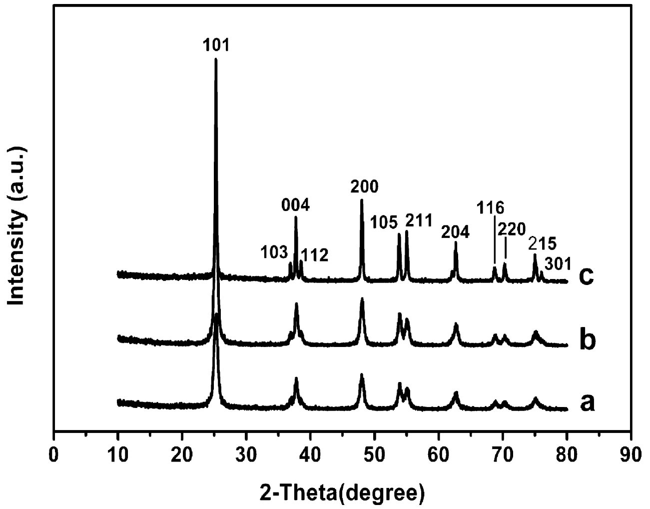

Fig. 3. XRD patterns of samples prepared by PEG 600 at different calcination temperatures (a) 450 °C; (b) 500 °C; (c) 600 °C.

the mesopores is composed of anatase nanocrystals. Thus HRTEM and XRD indicate the presence of mesopore network with a highly crystalline matrix between the mesopores. The corresponding well-defined selected-area electron diffraction (SAED) pattern of the aggregates of TiO_2 nanoparticles in Fig. 6c is indicative of high nanocrystallinity of the product and can be assigned to the anatase phase of TiO_2 [37].

3.5. Chemical reactions mechanism for the formation of porous structure

The chemical behavior of the titanium alkoxides precursor solution containing organic polymer such as PEG is very complex. Such reactions produce polycondensates whose chemical compositions are the function of their physical size and polymeric morphology. This situation arises from the fact that, during the hydrolytic condensation, an inorganic–organic network is formed by a chain of hydrolysis and polymerization reactions.

The reaction mechanism is proposed for the synthesis of mesoporous titania. During the first step of preparation method, $Ti(OBu)_4$ is added in acetic acid solution to make a solution A. Acetic acid forms complex with $Ti(OBu)_4$ according to the Eq. (1) in Scheme 1. Furthermore, in the second step of preparation, the solution B (the ethanolic solution of PEG) was added in solution A. Fig. 7 shows the FT-IR of sol after mixing the solution A and solution B. The presence of strong absorption peaks due to the esterification of carboxylic acid in the spectral region of 1115, 1240 and 1733 cm^{-1} demonstrates the above interactions in the titanium sol [38]. In the FT-IR spectrum, the absence of –COOH vibration band at 1700 cm^{-1} and the appearance of Ti–O–Ti at 1549 cm^{-1} proves that HAc has complexed with $Ti(OBu)_4$ according to Eq. (1). Then the hydrolysis and polycondensation reactions of $Ti(OBu)_4$ precursor occurred, the process can be written as below in Eqs. (2) and (3) of Scheme 1.

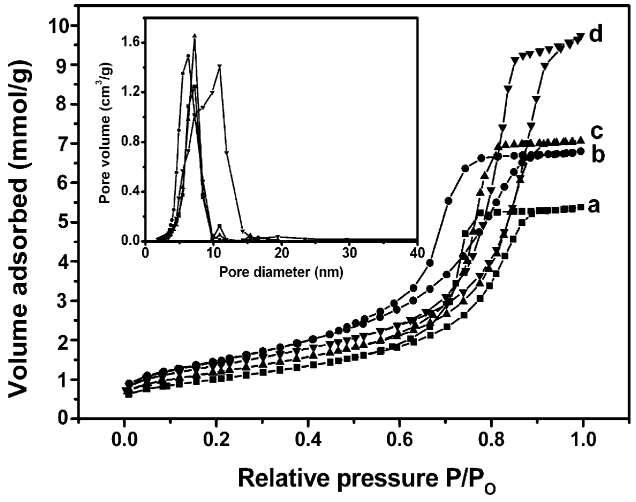

Fig. 4. N_2 adsorption–desorption isotherms and pore size distribution of mesoporous-TiO_2 samples with different molecular weights of PEG calcined at 450 °C (a) PEG 600; (b) PEG 2000; (c) PEG 10,000; (d) PEG 20,000.

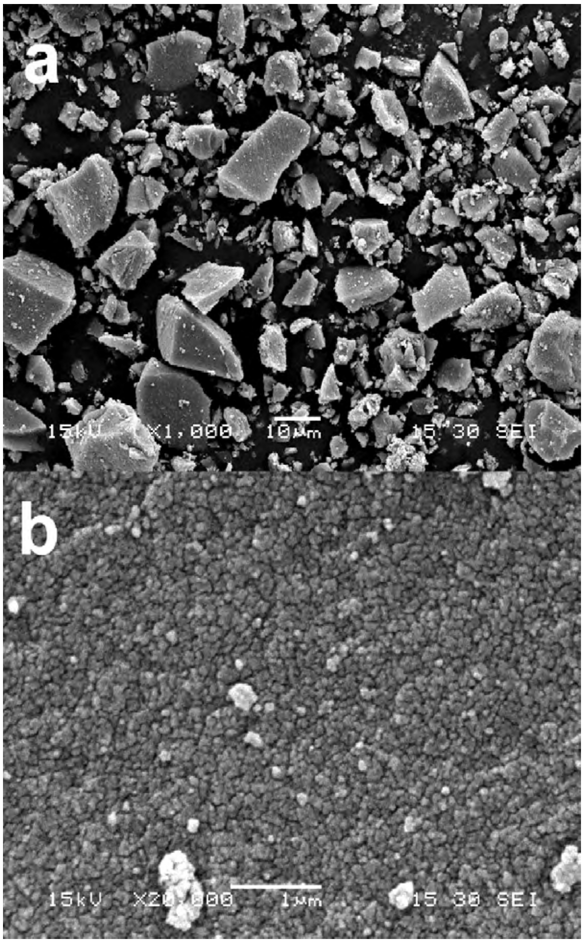

Fig. 5. Mesoporous-TiO_2 prepared by PEG 600 calcined at 450 °C (a) SEM image and (b) FESEM.

During reaction it implies that some polycondensations have occurred between PEG and the complex products, generating C_4H_9OH as shown in Eq. (4) of Scheme 1. PEG in the obtained inorganic–organic network configuration plays a role as the structure-directing agent leading to the original morphology for porosity of TiO_2 [39,40].

3.6. Photocatalytic degradation of chloro-phenol

The efficiency of catalysts was evaluated by using chloro-phenol as a model pollutant. No detectable degradation of chloro-phenol was observed without catalyst. The photocatalytic activity of mesoporous-TiO_2 nanoparticles prepared with different molecular weight PEG and Degussa P-25 was compared. The adsorption and removal efficiencies of chloro-phenol are displayed in Fig. 8(a) and (b). Fig. 8 shows the adsorption and degradation efficiencies of chloro-phenol increased with increasing PEG molecular weight.

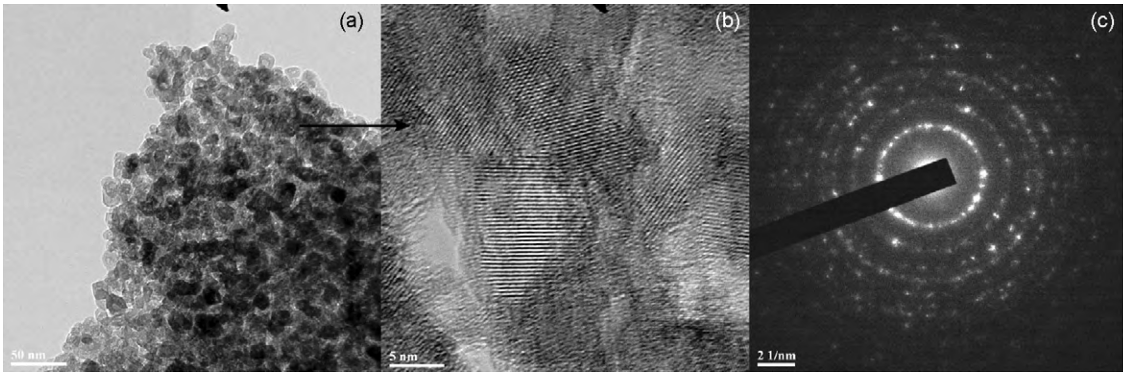

Fig. 6. Mesoporous-TiO_2 prepared by PEG 600 calcined at 450 °C (a) TEM image; (b) HRTEM; (c) SAED.

These photocatalysts exhibited far superior photocatalytic activity as compared to Degussa P-25. As the molecular weight of PEG increases the adsorption and degradation efficiencies of chlorophenol also increase. When PEG molecular weight was increased from 600 to 20,000, the degradation efficiencies were increased from 85 to 95%. The increase in the adsorption and photocatalytic efficiencies is attributed to the decreased crystalline size of synthesized mesoporous-TiO_2 and the increased mesoporous parameters such as the mean pore size, BET surface area and the pore volume (Table 1). The variations of the mesoporous structure parameters and the photocatalytic activity of synthesized mesoporous-TiO_2 may reflect some changes in configuration of ethylene chain in the PEG matrix in accordance with the molecular weight of PEG [5]. When the molecular weight of PEG exceeds 400, the PEG chain may be twisted and the PEG segments can form crown-ether-type complexes with inorganic ions through

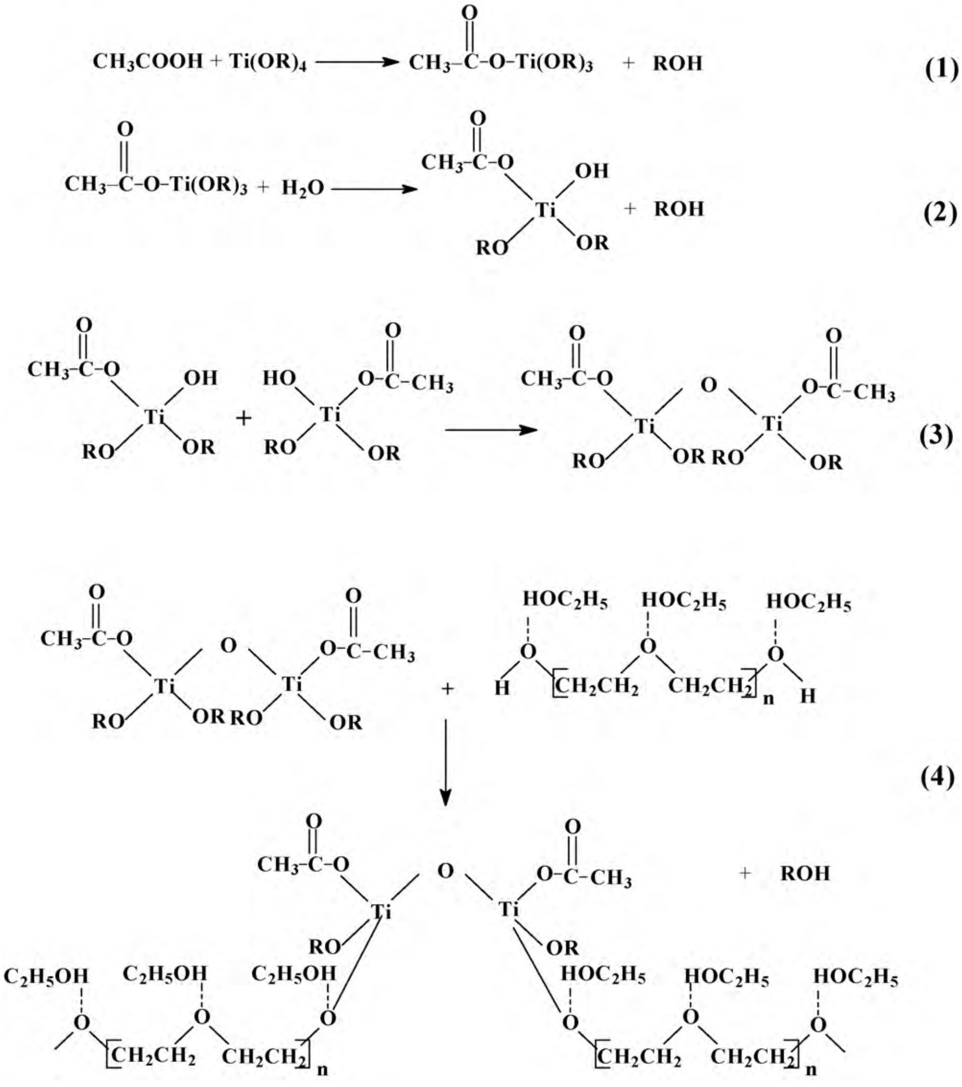

Scheme 1. Chemical mechanism for the formation of porous structure (R represent C_4H_9).

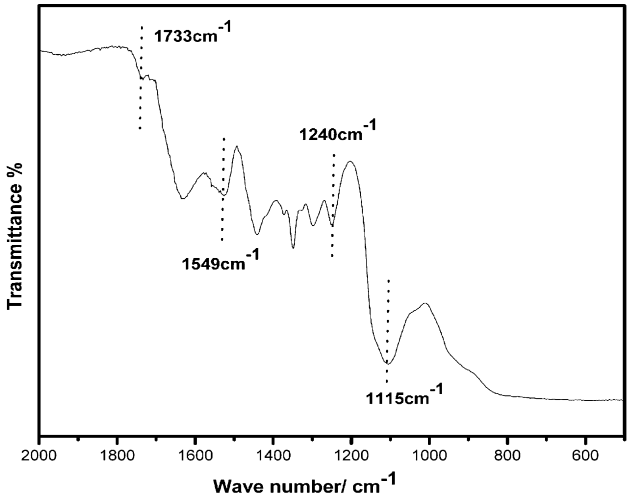

Fig. 7. FT-IR of sol after mixing the solution A (TBT + HAc) and solution B (ethanolic solution of PEG) for 2 h.

weak coordination interactions [3,15]. During the aging process, PEG molecules lose their bonding water which produce free PEG molecules available to form tightly "particles-PEG" complexes [3]. Thus a larger PEG molecule would result in a smaller crystalline size and larger mean porous size, BET areas and total volume which in turn would lead to enhanced adsorption and degradation efficiencies [41]. Fig. 9 shows the degradation profiles of chloro-phenol obtained from mesoporous-TiO_2 prepared at different thermal treatment temperatures. It is found that the chloro-phenol degradation efficiency increases as the sample calcination temperatures increase from 450 to 500 °C and then sharply decreases with further increase in calcination temperature to 600 °C.

A study of the effect of initial chloro-phenol concentration allowed us to define the optimal concentration field for photo-catalytic degradation practice. Fig. 10 shows the decrease of chloro-phenol concentration as a function of time for the experiments conducted at different initial concentrations of chloro-phenol. From the plot, it was observed that the degradation rate increased with increase in concentration of chloro-phenol up to 50 mg L^{-1} and then decreased. 10 and 25 mg L^{-1} of chloro-phenol were degraded 100% in 2 and 3 h, respectively. 50 and 100 mg L^{-1} were degraded 87 and 58% in 5 h, respectively. A plausible explanation of this behavior is that more and more organic substances are adsorbed on the surface of TiO_2 as the initial concentration increases, but the intensity of light and illumination time remains constant. Consequently, the $OH^{\bullet}$ formed on the surface of TiO_2 remain constant but the relative number of $OH^{\bullet}$ attacking the chloro-phenol decreases, thus the photodegradation efficiency also decreases [42].

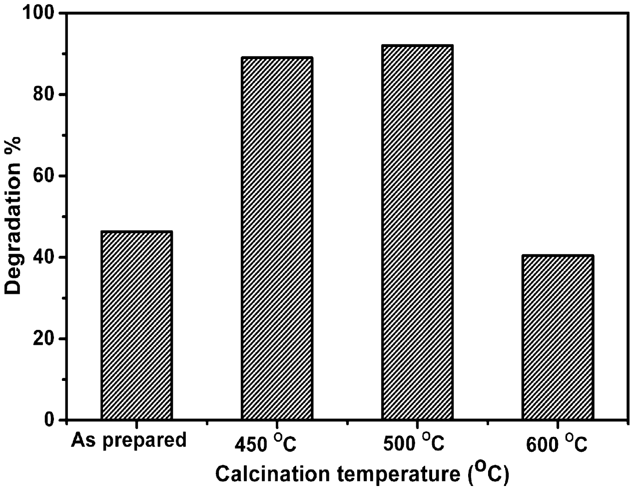

Fig. 9. Degradation of mesoporous-TiO_2 prepared by PEG 600 at different calcination temperatures [chloro-phenol]$_o$ = 50 mg L^{-1}.

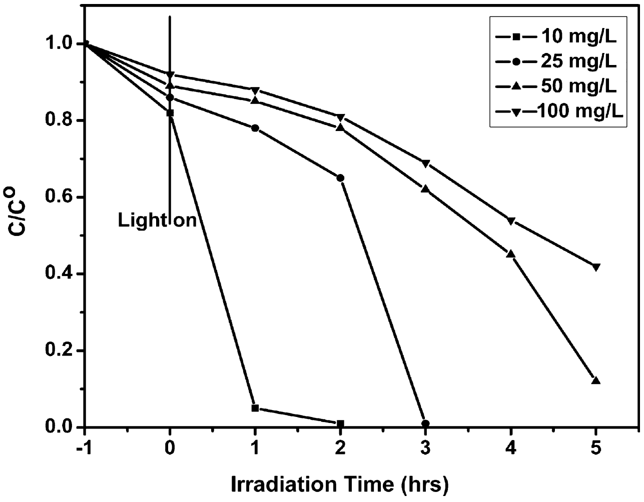

Fig. 10. Time dependent graph with initial concentration of chloro-phenol.

3.7. Mechanism of photodegradation

The photocatalytic oxidation of chloro-phenol involves complicated multistage processes. It has been demonstrated that the

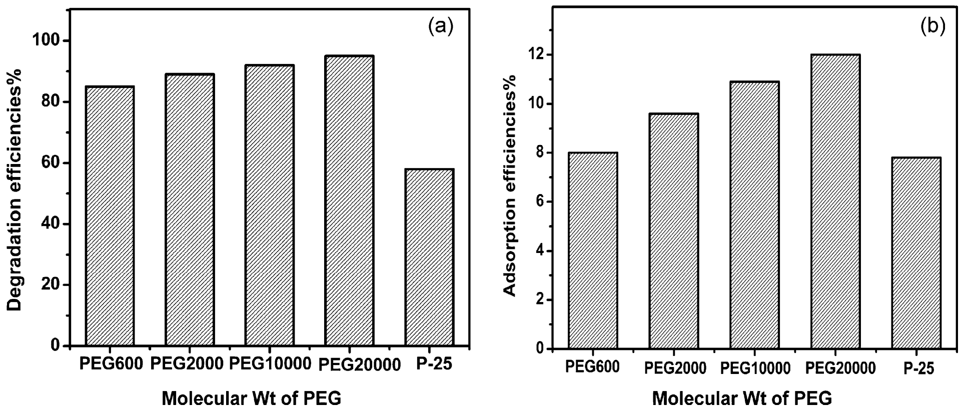

Fig. 8. Degradation and adsorption profile of mesoporous-TiO_2 calcined at 450 °C with PEG of different molecular weights [chloro-phenol]$_o$ = 50 mg L^{-1}.

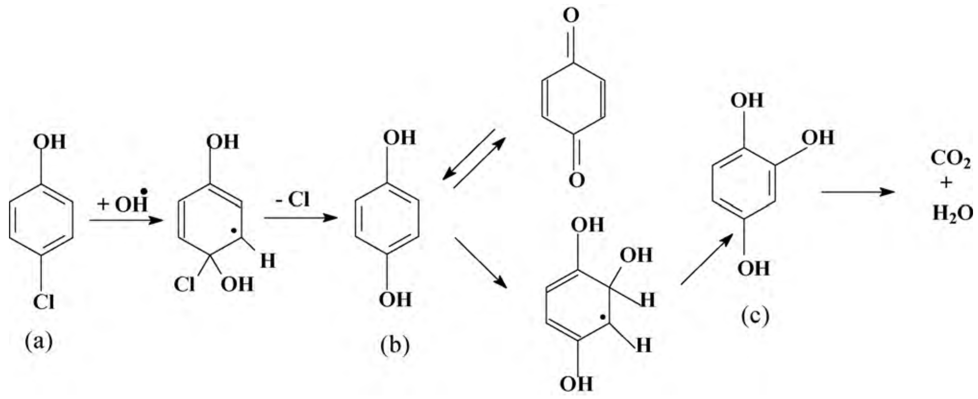

Scheme 2. The mechanism of chloro-phenol degradation (a) chloro-phenol; (b) dihydroxy-benzene; (c) hydroxy-hydroquinone.

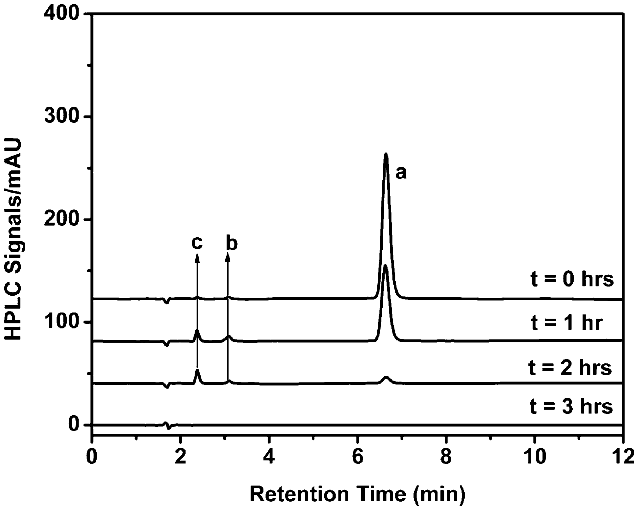

Fig. 11. HPLC of degradation of chloro-phenol by mesoporous-TiO_2 prepared using PEG 600 [chloro-phenol]$_o$ = 25 mg L^{-1}.

photocatalytic process with TiO_2 is energetically favorable for the decomposition of phenolic compounds. Two types of oxidizing species hydroxyl radicals and positive holes are involved in the transformation of aromatic compounds in oxygenated aqueous TiO_2 suspensions [43].

In most of the proposed mechanisms of TiO_2-mediated photocatalytic degradations of organic pollutants, the highly oxidizing (surface-bound) hydroxyl radicals which originate from the oxidation of chemisorbed –OH or H_2O by photo-generated valence band holes, are the main oxidative species responsible for the degradation [42]. The strongest evidence for the $OH^\bullet$ radical attack mechanism is formation of hydroxylated intermediates through addition of hydroxyl groups to aromatic rings during degradation process. The direct hole-organic reactions generate cation radicals which may be subsequently hydrated to generate hydroxylated products [44].

Various aromatic intermediate products are formed in the initial stage. These intermediate products then undergo further photocatalytic oxidation and finally degrade to CO_2 and H_2O. Scheme 2 shows the detected intermediates of chloro-phenol degradation by HPLC data. By comparison of retention time (RT) with the standard components, chloro-phenol (peak a with RT 6.7 min), hydroxy-hydroquinone (peak b with RT 3.3 min) and dihydroxy-benzene (peak c with RT 3.0 min) are the main intermediates identified. Because no other intermediates (e.g. aliphatic acids) are observed. It appears that the above mentioned intermediates further degrade to more polar compounds and eventually degrade to CO_2 [45–47]. Further degradation of the intermediates is likely via several reaction pathways that are simultaneously operative. An HPLC graph shown in Fig. 11 illustrates the removal of intermediates and chloro-phenol concentrations with the irradiation time. The photodegradation pathway proposed in Scheme 2 is consistent with the results of other research groups with anatase TiO_2 nanoparticles as catalyst [46,47].

4. Conclusions

The mesoporous-TiO_2 was successfully synthesized using PEG as template and acetic acid as hydrolytic retardant. It was observed that PEG was highly suitable template and allowed the preparation of mesoporous anatase with high crystallinity. The effect of PEG molecular weights was studied on the catalyst structural parameters and photocatalytic activities. As the molecular weight of PEG increased, the crystallinity, surface area, pore size and pore volume were also increased. The mechanism of the reaction during formation of mesoporous-TiO_2 was also proposed on the basis of FT-IR data. It was found that mesoporous-TiO_2 could be synthesized with good crystallinity using PEG as a template, $Ti(OBu)_4$ as a precursor and acetic acid as hydrolytic agent. The porous structure of TiO_2 was found to depend on the synthesis conditions. When mesoporous-TiO_2 samples were employed as photocatalyst for chloro-phenol degradation, degradation efficiencies increased with PEG molecular weights. The remarkably high catalytic activity of the mesoporous-TiO_2 was derived from its high crystallinity and mesostructure as compared to Degussa P-25. The mechanism for chloro-phenol degradation was also proposed on the basis of HPLC data.

Acknowledgment

This work has been supported by National Nature Science Foundation of China (20773039, 20977030); National Basic Research Program of China (973 Program, 2007CB613301, 2010CB732306), and the Ministry of Science and Technology of China (2007AA05Z303) and the Fundamental Research Funds for the Central Universities. Shamaila Sajjad and Sajjad Ahmed Khan Leghari thank Higher Education Commission (Pakistan) for support.

References

[1] C.T. Kresge, M.E. Leonowicz, W.J. Roth, J.C. Vartuli, J.S. Beck, Nature 359 (1992) 710–712.
[2] S. Shamaila, A.K.L. Sajjad, F. Chen, J. Zhang, Appl. Catal. B: Environ. 94 (2010) 272–280.
[3] L. Zhang, Y. Zhu, Y. He, W. Li, H. Sun, Appl. Catal. B: Environ. 40 (2003) 287–292.

[4] H. Zhao, D. Jiang, S. Zhang, W. Wen, J. Catal. 250 (2007) 102–109.
[5] G.S. Devi, T. Hyodo, Y. Shimizu, M. Egashira, Sens. Actuators B: Chem. 87 (2002) 122–129.
[6] J.H. Park, S.Y. Jung, R. Kim, N.-G. Park, J. Kim, S.-S. Lee, J. Power Sources 194 (2009) 574–579.
[7] L. Liu, J. Qian, B. Li, Y.M. Cui, X.F. Zhou, X. Guo, W.P. Ding, Chem. Commun. 46 (2010) 2402–2404.
[8] L. Yang, Y. Wang, D. Huang, G. Luo, Y. Dai, Ind. Eng. Chem. Res. 46 (2007) 579–583.
[9] Y. Chen, D.D. Dionysiou, Appl. Catal. A: Gen. 317 (2007) 129–137.
[10] R. Tan, Y. He, Y. Zhu, B. Xu, L. Cao, J. Mater. Sci. 38 (2003) 3973–3978.
[11] G.J.d.A.A. Soler-Illia, A. Louis, C. Sanchez, Chem. Mater. 14 (2002) 750–759.
[12] J.C. Yu, L. Zhang, J. Yu, New J. Chem. (2002) 416–420.
[13] K.S. Yoo, T.G. Lee, J. Kim, Micropor. Mesopor. Mater. 84 (2005) 211–217.
[14] S. Yuan, Q. Sheng, J. Zhang, F. Chen, M. Anpo, Q. Zhang, Micropor. Mesopor. Mater. 79 (2005) 93–99.
[15] J. Jiao, Q. Xu, L. Li, J. Colloid Interface Sci. 316 (2007) 596–603.
[16] H.X. Li, Z.F. Bian, J. Zhu, D.Q. Zhang, G.S. Li, Y.N. Huo, H. Li, Y.F. Lu, J. Am. Chem. Soc. 129 (2007) 8406–8407.
[17] D.M. Antonelli, J.Y. Ying, Angew. Chem. Int. Ed. Engl. 34 (1995) 2014–2017.
[18] A.S. Sawhney, C.P. Pathak, J.J. Van Resburg, R.C. Dunn, J.A. Hubbell, J. Biomed. Mater. Res. 28 (1994) 831–838.
[19] A.S. Sawhney, C.P. Pathak, J.A. Hubbell, Macromolecules 26 (1993) 581–587.
[20] H. Sertchook, H. Elimelech, C. Makarov, R. Khalfin, Y. Cohen, M. Shuster, F. Babonneau, D. Avnir, J. Am. Chem. Soc. 129 (2007) 98–108.
[21] L. Yang, Y. Wang, G. Luo, Y. Dai, Micropor. Mesopor. Mater. 94 (2006) 269–276.
[22] S.R. Zhai, C.S. Ha, Micropor. Mesopor. Mater. 102 (2007) 212–222.
[23] S.R. Zhai, C.S. He, D. Wu, Y.H. Sun, J. Non-Cryst. Solids 353 (2007) 1606–1611.
[24] K. Yu, J. Zhao, X. Zhao, X. Ding, Y. Zhu, Z. Wang, Mater. Lett. 59 (2005) 2676–2679.
[25] Y. Saito, S. Kambe, T. Kitamura, Y. Wada, S. Yanagida, Sol. Energy Mater. Sol. Cells 83 (2004) 1–13.
[26] Y.M. Cui, L. Liu, B. Li, X.F. Zhou, N.P. Xu, J. Phys. Chem. C 114 (2010) 2434–2439.
[27] B. Wen, C. Liu, Y. Liu, J. Photochem. Photobiol. A: Chem. 173 (2005) 7–12.
[28] X.H. Hu, T.C. An, M.L. Zhang, G.Y. Sheng, J.M. Fu, Res. J. Chem. Environ. 11 (2007) 13–21.
[29] X.J. Ding, T.C. An, G.Y. Li, S.Q. Zhang, J.X. Chen, J.M. Yuan, H.J. Zhao, H. Chen, G.Y. Sheng, J.M. Fu, J. Colloid Interface Sci. 320 (2008) 501–507.
[30] S. Vollmuth, A. Zajc, R. Niessner, Environ. Sci. Technol. 28 (1994) 1145–1149.
[31] B.T. Holland, L. Abrams, J. Stein, Am. Chem. Soc. 121 (1999) 4308–4309.
[32] T. Sen, G.J.T. Tiddy, J.L. Casci, M.W. Anderson, Chem. Mater. 16 (2004) 2044–2054.
[33] D.S. Kim, S.Y. Kwak, Appl. Catal. A: Gen. 323 (2007) 110–118.
[34] L. Liu, Y.M. Cui, B. Li, X.F. Zhou, W.P. Ding, Appl. Surf. Sci. 256 (2010) 2596–2601.
[35] H.P. Klug, L.E. Alexander (Eds.), X-ray diffraction procedures for polycrystalline and amorphous materials. Wiley, New York, 1974.
[36] H. Hao, J. Zhang, Mater. Lett. 63 (2009) 106–108.
[37] J. Lee, M.C. Orilall, S.C. Warren, M. Kamperman, F.J. Disalvo, U. Wiesner, Nat. Mater. 7 (2003) 222–228.
[38] S.T. Oh, J.S. Choi, H.S. Lee, L. Lu, H.H. Kwon, I.K. Song, J.J. Kim, H.I. Lee, J. Mol. Catal. A: Chem. 267 (2007) 112–119.
[39] M.S.W. Vong, N. Bazin, P.A. Sermon, J. Sol–Gel. Sci. Technol. 8 (1997) 499–505.
[40] D. Ravaine, A. Seminel, Y. Charouilot, M. Vincens, J. Non-Cryst. Solids 82 (1986) 210–216.
[41] J.C. Yu, J. Yu, L. Zhang, W. Ho, J. Photochem. Photobiol. A: Chem. 148 (2002) 263–271.
[42] S. Goldstein, G. Czapski, J. Rabani, J. Phys. Chem. 98 (1994) 6586–6591.
[43] K.N. Agaveni, G. Sivalingam, M.S. Hegde, G. Madras, Environ. Sci. Technol. 38 (2004) 1600–1604.
[44] M. Fox, M. Dulay, Chem. Rev. 93 (1993) 341–357.
[45] X. Li, J.W. Cubbage, T.A. Tetzlaff, W.S. Jenks, J. Org. Chem. 64 (1999) 8509–8524.
[46] Y. Cheng, H. Sun, W. Jin, N. Xu, Chem. Eng. J. 128 (2007) 127–133.
[47] X. Li, J.W. Cubbage, W.S. Jenks, J. Org. Chem. 64 (1999) 8525–8536.